Supplemental Information

Supplemental Methods.

Primary antibodies.

Primary antibodies used for immunostainings were as follow: Sheep anti-mouse FOXC2 (AF6989, R&D Systems), Goat anti-mouse Integrin α9 (AF3827, R&D Systems), Goat anti-mouse LYVE-1 (AF2125, R&D Systems), Rat anti-mouse LYVE-1 (MAB2125, R&D Systems), Goat anti-human Prox1 (AF2727, R&D Systems), Rat anti-mouse CD31 (MEC13.3, Pharmingen BD Biosciences), mouse anti-mouse α Smooth muscle actin (M0851, clone 1A4, DAKO).

Legends of supplemental figures.

Figure S1: Analysis of lymphatic capillary vessel patterning in the skin of E15.5 embryos and P0 neonates. Left panels: LYVE-1 whole mount immunostainings of ventral skin of P0 neonates. Representative images of P0 ventral skin lymphatic capillaries are shown. Quantification of the mean LYVE-1-positive area is expressed as percentage of the total area measured using Image J software. Values are the mean ± SE; n = 7 (*Bmp9*-KO) or n = 8 (WT). **P≤0.01, significantly different from WT pups by unpaired Student' *t* test. Right panels: LYVE-1 whole mount immunostainings of dorsal skin of E15.5 embryos. Representative images of skin along the dorsal midline are shown. Quantification of sprouting was performed by counting the number of tips per surface area kept constant in all images and placed along the lymphatic front migration. Values are mean ± SE; n = 9 (*Bmp9*-KO) or n = 5 (WT). ns, not significant by unpaired Student' *t* test.

Figure S2: Absence of blood vessel abnormalities in *Bmp9*-KO mice.

Representative images of CD31 whole mount immunostainings of P0 neonate ventral skin and of adult ear skin for both WT and *Bmp9*-KO mutants are illustrated. In both cases, the mean CD31-positive area was measured using Image J software on at least 3 randomly selected fields. Data are the mean ± SE; n = 3 for each genotype at P0; n = 9 (*Bmp9*-KO) or n = 7 (WT) for adult ear skin. ns; not significant by unpaired Student' *t* test.

Figure S3: Analysis of valve stage III/IV integrity in P4 *Bmp9*-KO neonates.

Lymphatic mesenteric collecting vessels from P4 WT or *Bmp9*-KO neonates were immunostained for FOXC2 (green) and CD31 (red), Integrin α9 (green) and CD31 (red), or Prox1 (green) and αSMA (red). Representative images of valves at stage III/IV are illustrated. The arrows point to the valves.

Figure S4: Defective lymphatic valve formation in the diaphragm of adult *Bmp9*-KO mice.

A, B and C; Representatives images of CD31 and Prox1 whole mount immunostainings of a lymphatic valve in the diaphragm of a WT mouse. The arrowhead points to the valve location. D and E; visualization of lymphatic valves after CD31 whole mount immunostaining. Representative images of lymphatics in the tendinous region of the diaphragm of WT and *BMP9*-KO deficient mice are shown. The arrows point to valves. Note the presence of enlarged vessels in the *Bmp9*-KO mutant. F; Quantification of valve number per unit of lymphatic vessel length. Counts were performed on the entire lymphatic vessel network of the tendinous region of the diaphragm. Values are mean ± SE; n = 5 for each genotype. ***P≤0.001, significantly different from WT by unpaired Student' *t* test.

Figure S5: Evans blue labeling of lymph nodes (LN) and of the hindlimb lymphatic collecting vessels in WT and *Bmp9*-KO adult mice.

A, B; The popliteal LN (white arrow) is labeled after left hindfoot injection (blue arrow) of 3 µl 3% Evans Blue. Note the diffusion of the dye in the remaining skin of the limb in the *Bmp9*-KO mutant, reflecting a poor draining efficiency. C, D; High magnification of the popliteal region of a right hindlimb showing dye labeling of the popliteal LN (white arrow) and of the afferent lymphatic collecting vessels (white arrowheads). E, F; Inguinal LNs (left flank) are labeled after injection of 5 µl 3% Evans Blue dye into the lateral tail base. The asterisk points to the inguinal LN and the black arrow indicates the efferent lymphatic vessel that drains to the axillary LN. Note the stronger labeling in the WT compared to the *Bmp9*-KO mutant. In all experiments, mice were sacrificed 20 min after Evans Blue injection.

Figure S6: **Distribution of FITC-Dextran after injection into the hind limb footpads of WT and *Bmp9*-KO neonates.**

1.5 µL of 5 mg/mL FITC-Dextran (MW: 2000 kDa, Sigma) diluted in PBS were injected into the hind limb footpads of anaesthetized P4 or P5 neonates. After 15 min, the pups were sacrificed by decapitation and the skin overlaying the limb was carefully removed by dissection and layered out. The lymphatic vessel networks of both the skinned limbs and the removed skin were imaged with a fluorescence macroscope (LEICA CLS 150X) equipped with an ORCA C9100 camera (Hamamatsu). Image analysis was performed with Wasabi 1.5 software (Hamamatsu).

A and B, Visualization of the deep collecting lymphatic vessels of the calf (arrows) and of the popliteal lymph node (yellow asterisk). C and D, Distribution of the dye in the superficial dermal lymphatic capillary network of the calf skin. E and F, High magnification of the central areas of images C and D (box).

<u>Supplemental Table 1:</u> PCR Primer sets used for gene expression analysis.

Gene	Upstream primer	Downstream primer
LYVE-1	5’- AACAATAGGCTGCAAACTGTCGGC -3’	5’- AAACTTGCAGCTATGGCTGGGTTG -3’
Prox1	5’- TTGCCGGCTTAAGAGGGCTGTG -3’	5’- GCGCTCCGCTCCTCCCAGTT-3’
Foxc2	5'- CGGCTTCACCAGGTCCTTAG -3'	5'- GAGCCGTCTCGGAAGCAG -3'
Connexin37	5’- GGTCCAGCAACTTCTCCAGG -3’	5’- CATCGTCCCCACCTCCAC-3’
Neuropilin-1	5’- AAATGGCGCCCTGTGTCCCG -3’	5’- CAGAGCGCTCCCGCCTGAAC-3’
EphrinB2	5’- TCCAGGCCCTCCAAAGACCCA -3’	5’- CCCTCTCCTCAACTGTGCCAAACC -3’
Connexin43	5’- ACTTGGCGTGACTTCACTACT-3’	5’- CCAGCAGTTGAGTAGGCTTGA -3’
Semaphorin3a	5’- ATTTTGAAAACGGCCGTGGG-3’	5’- GTGCCCAAGAGTTCGGAAGA -3’
NFATc1	5’- GTCCTGGAGATCCCACTCCT -3’	5’- GTTCTTCCTCCCGATGTCCG -3’
Integrin α9	5’- GAGATGCACCGAACTGGACA -3’	5’- ATCCACTCATCATCGCGGTC -3’
HPRT	5’- GCTGGTGAAAAGGACCTCT -3’	5’-CACAGGACTAGAACACCTGC-3’

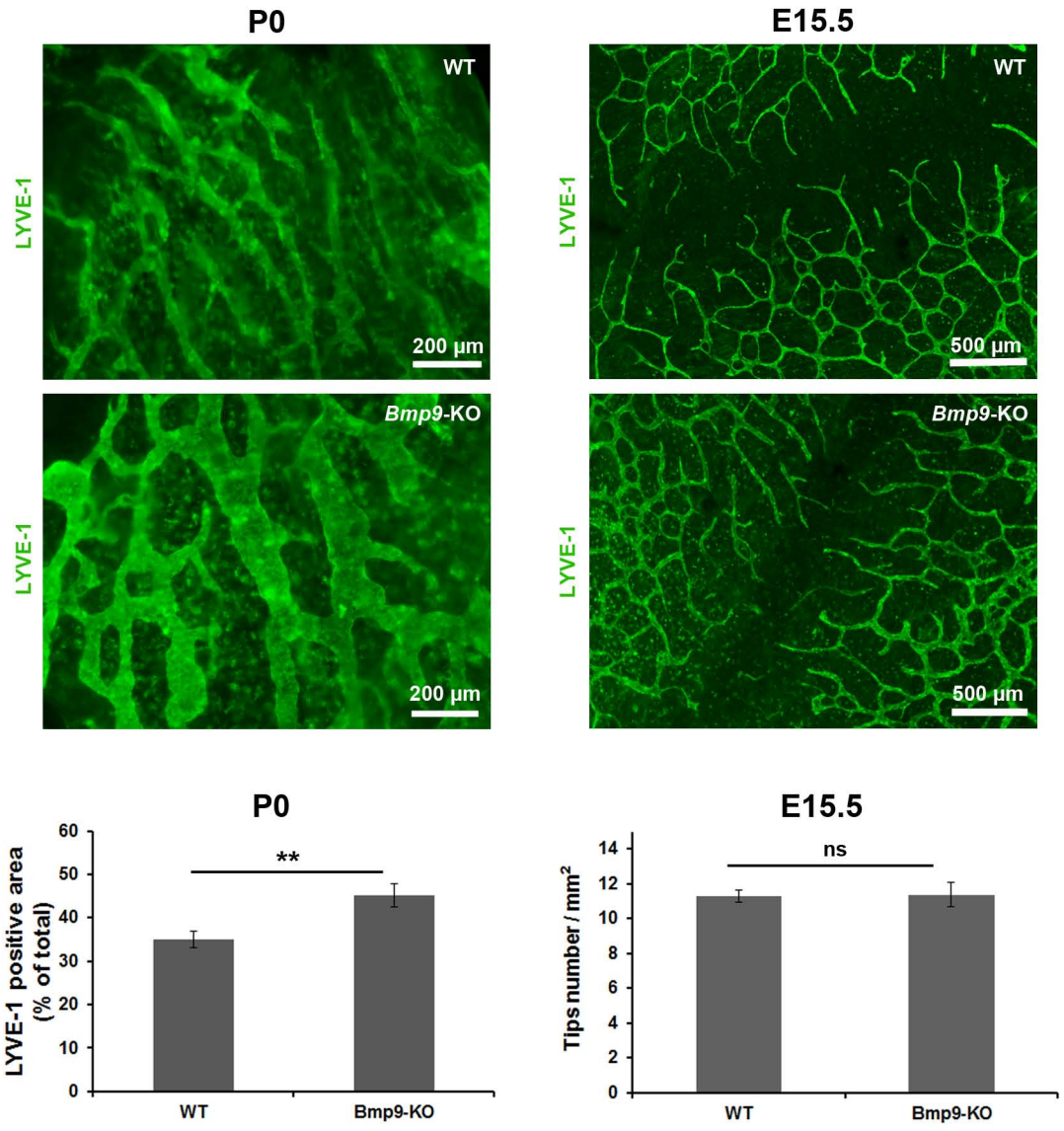

Figure S1

(Levet et al.)

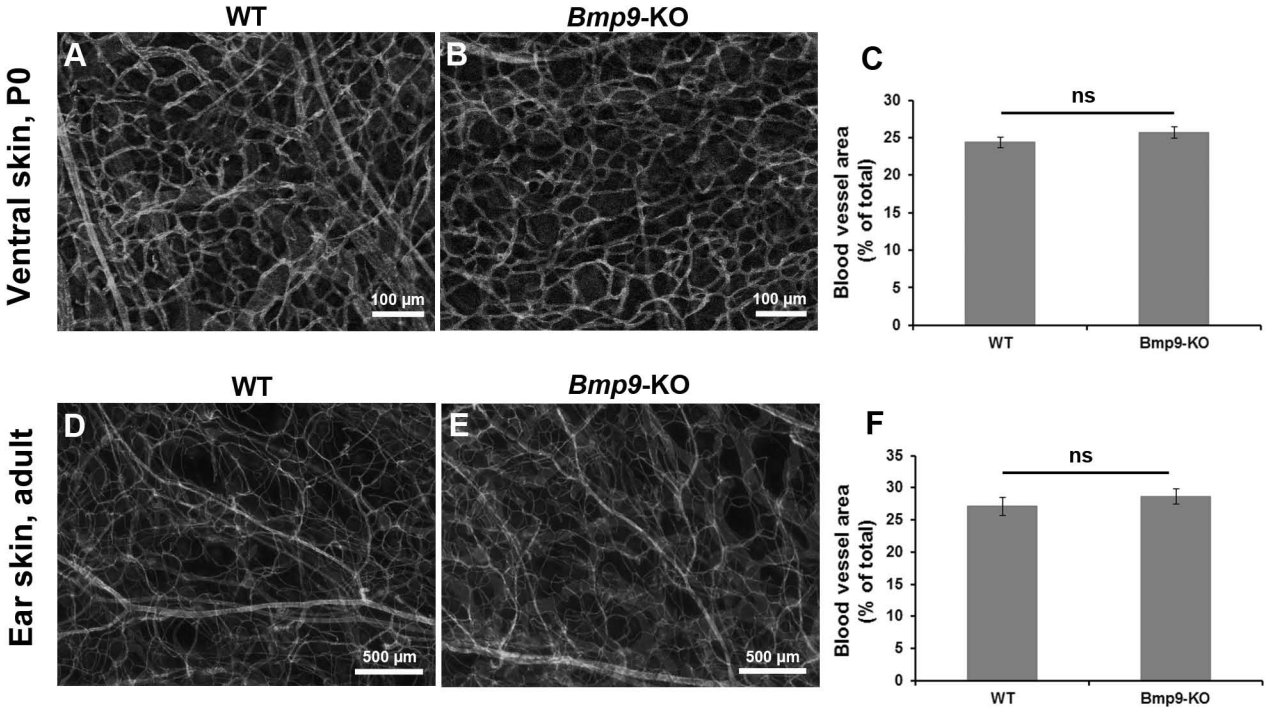

Figure S2

(Levet et al.)

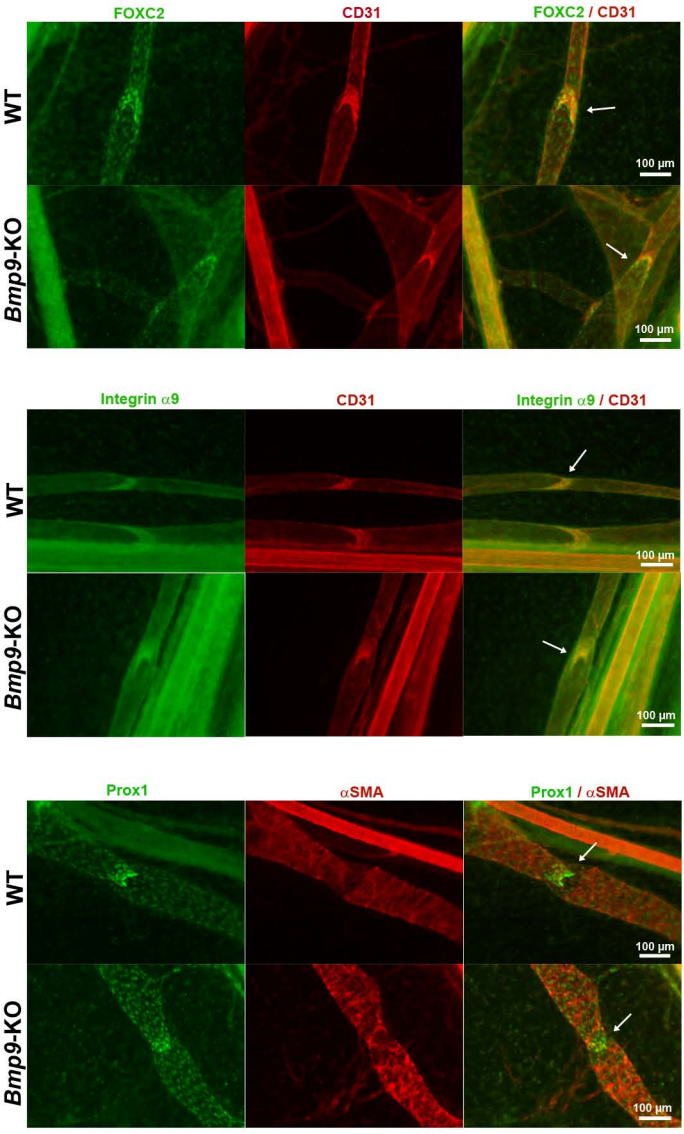

Figure S3

(Levet et al.)

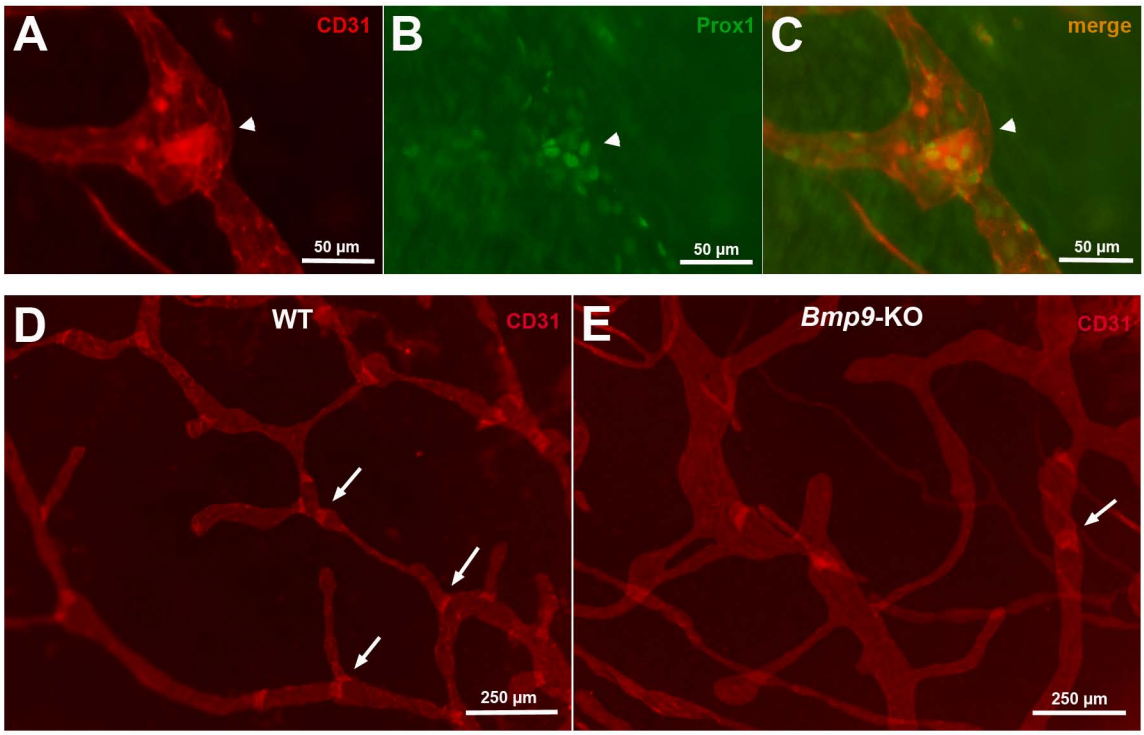

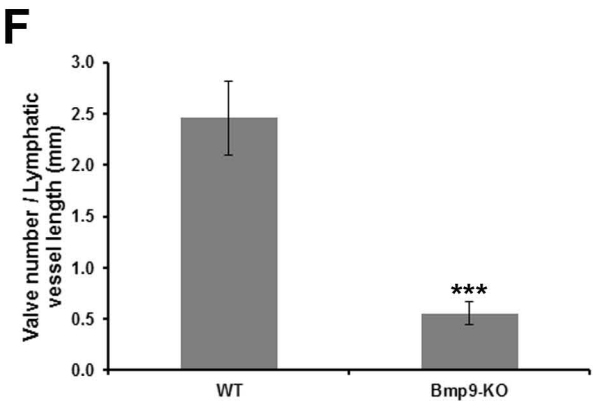

Figure S4

(Levet et al.)

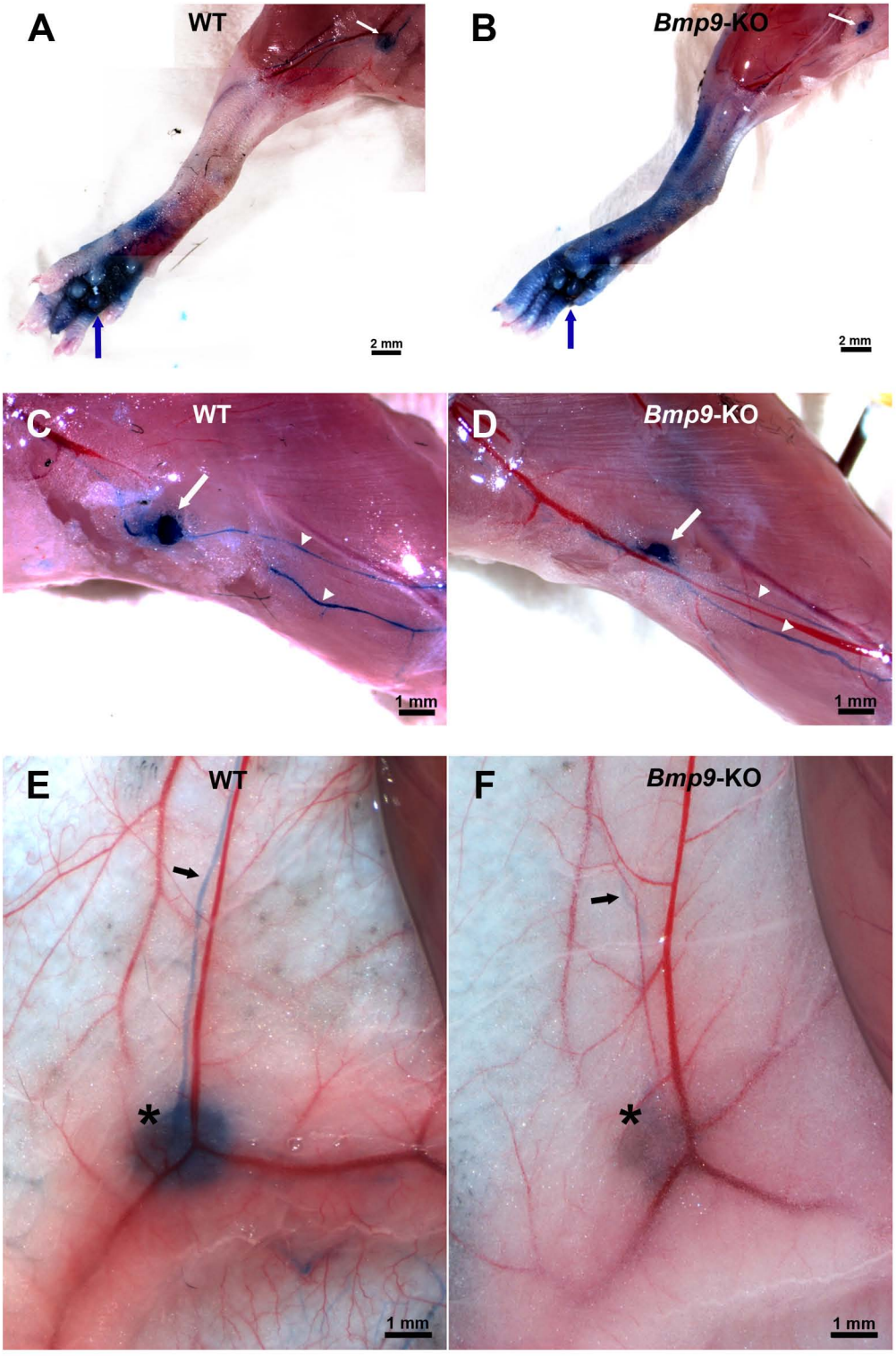

Figure S5

(Levet et al.)

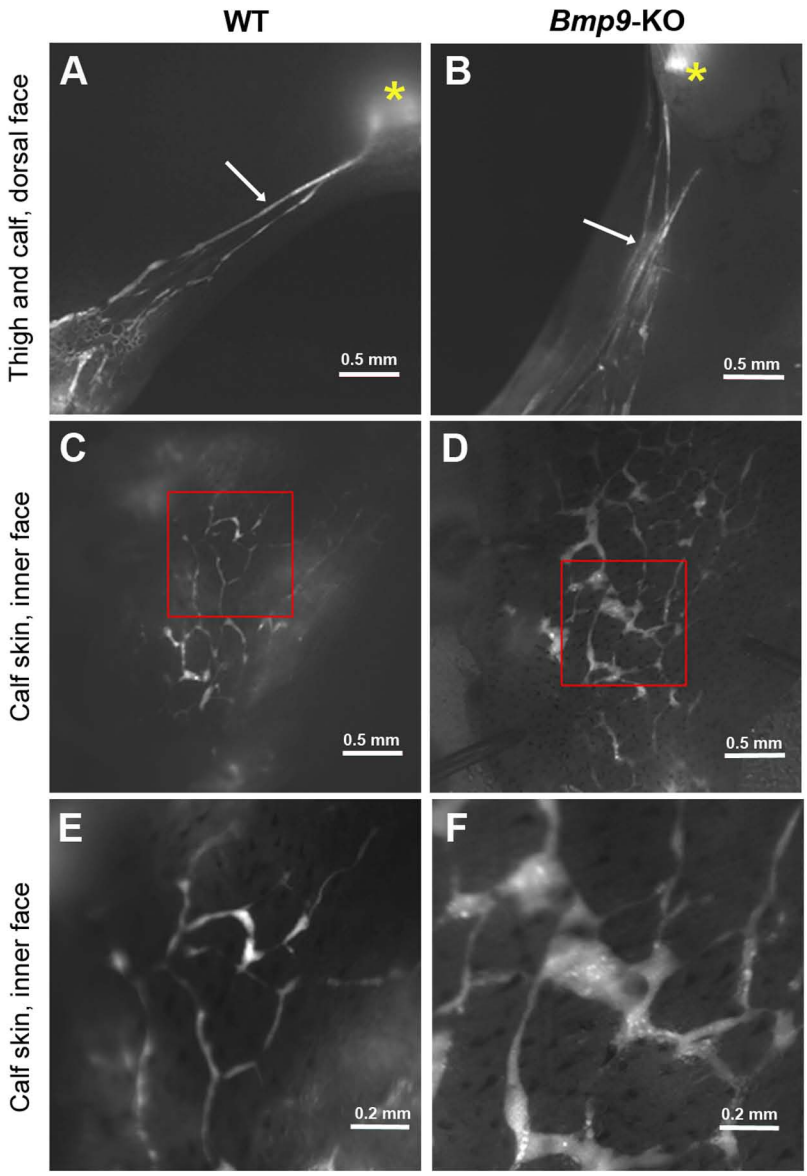

Figure S6

(Levet et al.)